Low-voltage cathodoluminescence of europium-activated yttrium orthovanadate

Mark L. F. Phillips

Sandia National Laboratories
Albuquerque, NM 87185

ABSTRACT

Emissive flat panel display systems operating in full color demand higher performance at low voltages (ca. 50-1000 V) from cathodoluminescent (CL) phosphors than cathode ray tubes require. Hydrothermal synthesis has been suggested as a route to phosphors with improved efficiencies, lower voltage thresholds, and increased saturation power. This hypothesis was tested in europium-doped yttrium orthovanadate (YVO_4:Eu), an efficient, red emitting CL phosphor. The CL efficiency of YVO_4:Eu crystallized from aqueous solution at 200 °C is relatively low until it is annealed. The distribution of particle sizes in the low-temperature phosphor is similar to that in material made via a solid-state route, but crystallites remain much smaller (ca. 400 Å) until they are annealed. These observations, along with the anomalously strong dependence of CL intensity on europium concentration, support a model in which efficiency principally depends on crystallite size. CL efficiency of both solid state and hydrothermal YVO_4:Eu increases with voltage at constant power. Surface-bound electrons are likely the dominant influence on efficiency at voltages near threshold. Saturation power is independent of synthetic route. It is apparent that the CL properties of hydrothermally synthesized YVO_4:Eu are essentially the same as those of YVO_4:Eu produced via conventional, high-temperature routes.

1. INTRODUCTION

By the end of this decade, annual sales of flat panel displays (FPDs) are expected to approach $20 billion.[1] The market in FPDs for portable computers is currently dominated by liquid crystal displays (LCDs). Significant growth is still expected in LCD sales, particularly those of active matrix LCDs. However, emissive FPD technologies such as field emitter (FED), electroluminescent (ELD), and vacuum fluorescent (VFD) displays are expected to compete with AMLCDs for use in portable monitors. A major issue driving these new display technologies is their lower manufacturing cost, since the cost of AMLCD displays is a large component of the price of portable computers.

In addition to lower manufacturing costs, full color FEDs are expected to realize lower power consumption and improved screen appearance. Like a conventional cathode ray tube (CRT), FEDs use electron beams to excite cathodoluminescent phosphors deposited on a screen. But while a color CRT forms an image by rastering beams from three thermionic electron guns scanning across a screen containing lines of red, green, and blue phosphors, a FED uses an array of microscopic cold cathodes to irradiate a phosphor screen. Such arrays can contain as many as 10^7 emitters/cm^2, so that thousands of emitters can be used to light a single pixel.[2]

A significant difference between the operation of a CRT and FED is voltage. The electron guns in CRT displays produce electrons at high energy (typically 10-25 keV). FEDs are operated at lower voltages for several reasons. Principally, the screen must be held a short distance (40-100 μm) from the cathode array to minimize cross-talk (unintentional irradia-tion of neighboring pixels). This causes a large potential gradient, and limits voltages to less than ca. 1000 V to prevent vacuum breakdown. In addition, supplying high operating voltages to 10^9 cathodes in a monitor screen would require costly, bulky driver circuitry, and could constitute a safety hazard.

A major drawback to using lower voltages is reduced phosphor performance. Most phosphors are inefficient at low voltages, principally due to surface bound electrons (SBEs) and surface recombinant (SR) centers. SBEs cause the surface of the phosphor grain to acquire a negative charge, which repels or deflects the incoming electrons. SR centers are surface defects at which excitons created by electron impact can decay nonradiatively; these can be caused by surface contamination or grinding.[3] Using higher current densities to compensate for loss of efficiency at low

TJ

excitation voltage can also lead to saturation and/or damage. Sulfide phosphors, which offer the highest luminescent efficiencies in full color, can release sulfur-containing gases under low-energy electron irradiance.[4] In addition to damaging the phosphor grain, degradation can contaminate the field emitter tips, changing their work functions and increasing or decreasing emission current.[5]

Oxide phosphors are cleaner, but the selection for those that are efficient at low voltages is scanty. ZnO:Zn is is unusual among oxide phosphors in that it is a conductor, rather than an insulator. Its visible cathodoluminescence is blue-green; efficiencies of up to 13 lm/W have been reported.[6] $ZnGa_2O_4$ is a candidate for a low-voltage blue phosphor.[7] Red oxide phosphors include traditional materials such as Y_2O_3:Eu, YVO_4:Eu, $Y_3Al_5O_{12}$ (YAG):Cr, $Zn_3(PO4)_2$:Mn, and some newer materials such as $CaTiO_3$:Pr.[8] So far, though, no obvious low-voltage red oxide phosphors have emerged.

Hydrothermal synthesis is a route to producing well-crystallized oxide powders with good control over particle size distribution. Among others, these criteria are key to optimizing phosphor performance.[9] Phosphors and host phases that have been synthesized hydrothermally include $Y_3Al_5O_{12}$ (YAG),[10] $ZnGa_2O_4$,[11] Zn_2SiO_4:Mn,[12] Y_2O_3,[13] and YVO_4:Eu.[14] The work reported here targets YVO_4:Eu because it is an efficient, red-emitting phosphor that is readily synthesized either hydrothermally or via traditional high temperature methods, making it a good model system for determining whether hydrothermal synthesis improves its low-voltage characteristics. Ropp states that the photoluminescent efficiency of hydrothermally-derived YVO_4:Eu exceeds that of YVO_4:Eu made via solid state routes at high temperature.[15]

Once a phosphor has been synthesized, it must be annealed for maximum brightness. Ropp reports that precipitated, unannealed YVO_4:Eu has brightness of about 40% of final, annealed product.[16] Ozawa states that the role of annealing is to improve crystal quality such that the probability of radiative transition of the excited activator ion (Eu^{3+}, in this case) is increased.[9] In addition to characterizing the low-voltage CL properties of this phosphor, a goal of this work is to correlate changes in structure upon annealing with luminescence. These were accomplished by synthesizing YVO_4:Eu over a range of activator concentrations, correlating changes in luminescence and structure with annealing temperature, understanding the relationship between CL intensity and activator concentration, and measuring CL efficiency as a function of excitation power and voltage.

2. EXPERIMENTAL

2.1. Synthesis

Samples of YVO_4:Eu were prepared by treating a mixture of $Y(NO_3)_3 \bullet 5H_2O$, $Eu(NO_3)_3 \bullet 6H_2O$, NH_4VO_3 and deionized water with a moderate alkali such as NH_4OH or guanidine carbonate ($(C(NH_2)_3)_2CO_3$) until the pH reached 11. The resulting suspension was held at 200 °C in a pressure vessel until it had fully crystallized. Products were recovered by filtration, and immersed in a 2% Na_2CO_3 solution at 90 °C for several hours to remove any excess V_2O_5. This process yielded white or cream-colored powders that were determined to be pure $(Y_{1-x}Eu_x)VO_4$ by powder X-ray diffraction. Products were annealed in Pt crucibles by heating to the desired annealing temperature, holding at that temperature for 3 hr., then cooling to 22 °C at a rate of 5 °C/min. Some powders were annealed at 1040 °C for 3 hr in sealed Au tubes.

Solid state YVO_4:Eu was prepared by grinding together Y_2O_3, Eu_2O_3, and NH_4VO_3, heating in an Al_2O_3 crucible at 800 °C for 18 hr, regrinding, and reheating at 1040 °C in sealed Au tubes for 18 hr. Excess V_2O_5 was removed by suspension in 2% Na_2CO_3 solution as above. The powders were then annealed in Al_2O_3 crucibles at 1150 °C for 3 hr, followed by cooling to room temperature at a rate of 5 °C/min.

2.2. Characterization

Particle sizes were determined by scanning electron microscopy (SEM) and by sedimentation. Samples for SEM were sputtered with Au, and analyzed using an AMRAY model 1645 electron microscope. Particle size determination by sedimentation was accomplished by suspending the powder samples in a sodium pyrophosphate solution, sonicating, and measuring settling rates using a Horiba CAPA-7000 particle size analyzer. Powder X-ray diffraction (XRD) data were collected using a Siemens D500 diffractometer. Crystallite sizes were calculated

from the width of the (101) line, using a LaB_6 standard. Thermogravimetric analysis data were collected using a Rheometrics STA 1500 thermal analyzer.

Fluorescence spectra were collected in reflectance, using a monochromated mercury lamp (253.7 nm line) as the excitation source. Cathodoluminescence experiments were conducted in a vacuum chamber evacuated to $3x10^{-8}$ torr. A hot filament, low-energy electron gun (Kimball Physics) was used as the source of the beam, which was steered and focused via external Helmholtz coils. The samples were packed into stainless steel cups. During analysis the sample cup was maintained at a potential of +30 V with respect to ground. The electron beam was focused onto a spot 4.5 mm in diameter; light emitted from the sample was transmitted to a spectroradiometer (Oriel), which measured radiant energy as a function of wavelength. A mass spectrometer (Ferran Scientific) was used to monitor the chamber for any vapor released by the sample during excitation.

CL intensity data are reported here as maximum radiance and as luminance. Luminance has the units of candela/m^2, and was determined by integrating spectral intensity from 400 to 800 nm. Radiance has the units of power per unit area per unit solid angle per nm of linewidth, and was measured at the λ_{max} of YVO_4:Eu (619 nm). Radiance data were more reliable at low intensities, where low signal/noise limited the precision of integrated intensity measurements.

3. RESULTS

Sedimentation data indicate that the sizes of the YVO_4:Eu particles prepared hydrothermally are somewhat smaller than those prepared via the solid state route. The mode of the particle size distribution of the powders prepared hydrothermally was 2 μm. Nearly half of the volume fraction of particles occurred at less than 1 μm, and this proportion increased with sonication time. This suggests that the particles are loosely constituted, and that they consist of clusters of much finer crystallites. The proportion of submicron particles diminishes significantly during annealing, indicating that the finer particles are probably sintering at annealing temperature. The mode of the particle size distribution for YVO_4:Eu made via the solid state route was at 5 μm. Fewer than 1% of particle volume was less than 2 μm in diameter. Either synthetic route yields YVO_4:Eu powders with particle sizes that are within the range used in CRT screens, though the hydrothermally prepared material may be more appropriate for screens requiring finer resolution or increased packing density.

SEM views corroborate this picture. These micrographs show that unannealed, hydrothermal YVO_4:Eu powder consists of irregular clumps with no distinct morphology (Figure 1). Individual crystallites begin to appear after the material is annealed at 1040 °C (Figure 2). These crystallites do not reach the size of solid state YVO_4:Eu particles (Figure 3) until annealed at 1150 °C (Figure 4).

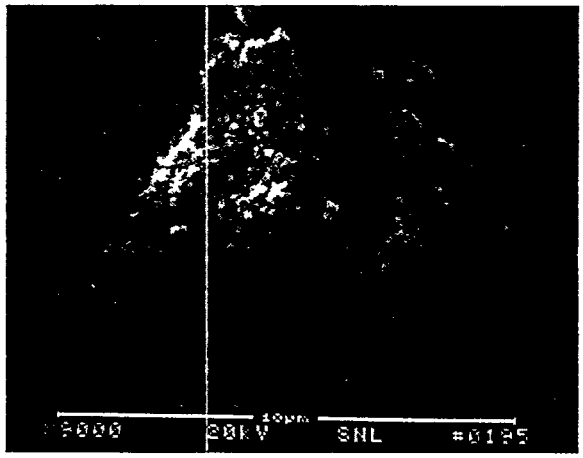

Figure 1: SEM photograph of YVO_4:Eu crystallized from aqueous solution at 200 °C.

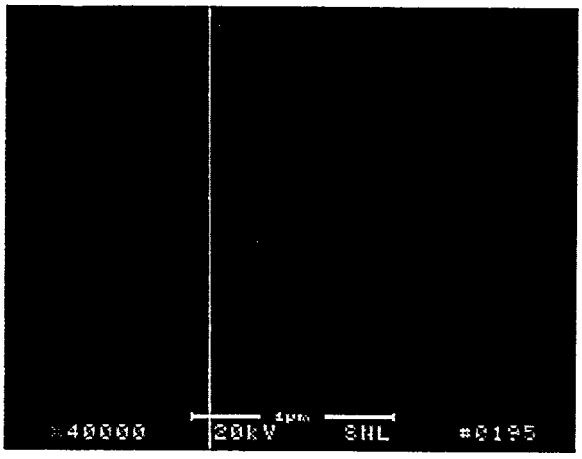

Figure 2: Hydrothermally crystallized YVO_4:Eu, annealed at 1040 °C.

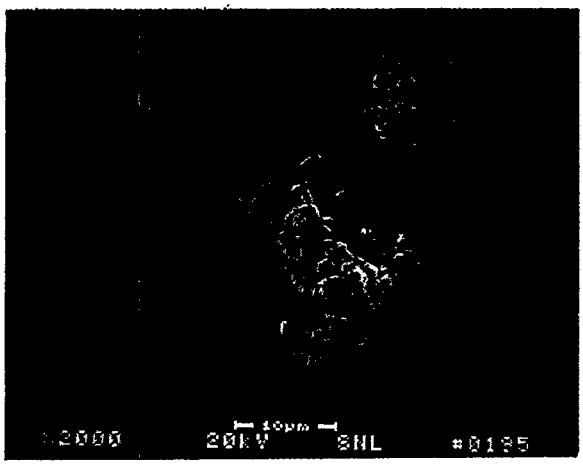

Figure 3: YVO_4:Eu made via solid state route, annealed at 1150 °C.

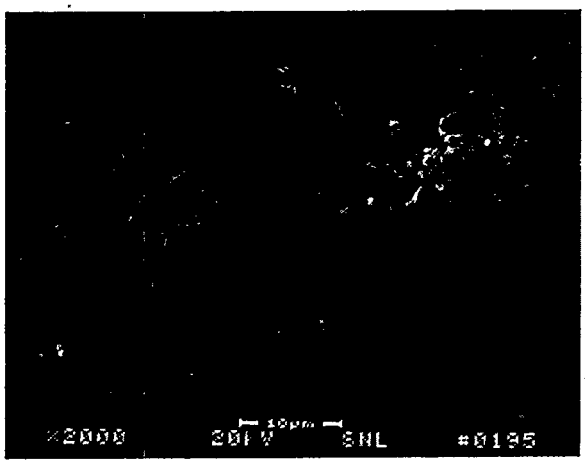

Figure 4: Hydrothermally crystallized YVO_4:Eu, annealed at 1150 °C.

Crystallite sizes in the precipitated YVO_4:Eu were calculated from powder XRD line widths, and are approximately 400 Å in diameter. The sizes of the crystallites do not approach that of the particles until the material is annealed above 1000 °C (Figure 5). Unannealed and annealed YVO_4 are crystallographically isomorphous, crystallizing in a tetragonal lattice structurally related to zircon ($ZrSiO_4$). The lattice parameters increase slightly upon annealing: for precipitated YVO_4:3% Eu, a = 7.0982(20), c = 6.2763(43), and for the annealed phosphor, a = 7.1236(3) , c = 6.2949(5).

Cathodoluminescent radiance at constant power increases with annealing temperature, as does crystallite size (Figure 5). Fluorescence intensity of

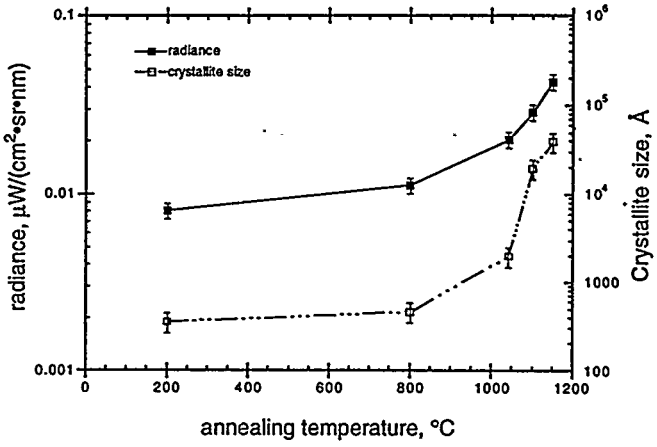

Figure 5: Maximum cathodoluminescent radiance and crystallite size of YVO_4:Eu as functions of annealing temperature.

precipitated YVO_4:Eu is typically about 30% of the final product (Figure 6), but the spectra appear identical otherwise, with very similar relative line intensities and peak widths at half maxima, and indistinguishable differences in peak positions. These data suggest that the crystal fields of the activator ions are essentially unchanged during annealing. It is conceivable that residual water may be present in microscopic crystal defects in the unannealed samples, quenching the activator and reducing luminescent efficiency. But thermogravimetric analysis of hydrothermal YVO_4:Eu shows a weight loss of less than 40 ppm between room temperature and 1000 °C, indicating that aqueous lattice defects are probably not an issue.

Figure 7 compares radiance maxima as functions of activator concentrations for unannealed hydrothermal, annealed hydrothermal, and solid state YVO_4:Eu, and Y_2O_3:Eu. The most obvious result is that the YVO_4:Eu becomes much more efficient after it is annealed, and at low Eu concentrations, brightness is increased tenfold. After annealing, the hydrothermal phosphor is approximately as luminous as the same composition made via solid state at the same temperature, within experimental error. At a given activator concentration, Y_2O_3:Eu is measurably brighter. It should be noted, though, that the cathodoluminescence spectra of Y_2O_3:Eu and YVO_4:Eu are slightly different ($\lambda_{max}Y_2O_3$:Eu = 611 nm), and the emission from the former material appears distinctly orange. Finally, while the

relationship between log (radiance) and log [Eu] is linear in all of the compositional series studied, the slopes of the high temperature sets are nearly identical (0.34), while the slope of the unannealed hydrothermal set is much steeper (0.61).

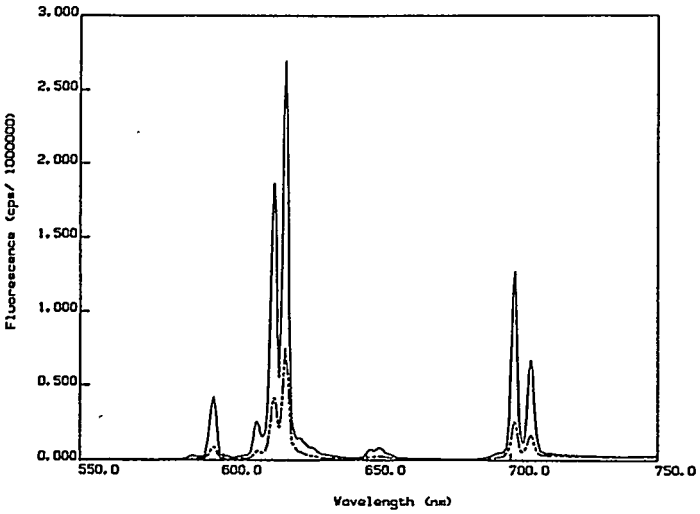

Figure 6. *a.* Fluorescence spectrum of unannealed hydrothermal YVO_4:3% Eu (dashed line). *b.* Spectrum of same composition, after annealing at 1150 °C. Both spectra were obtained using a 253.7 nm excitation source.

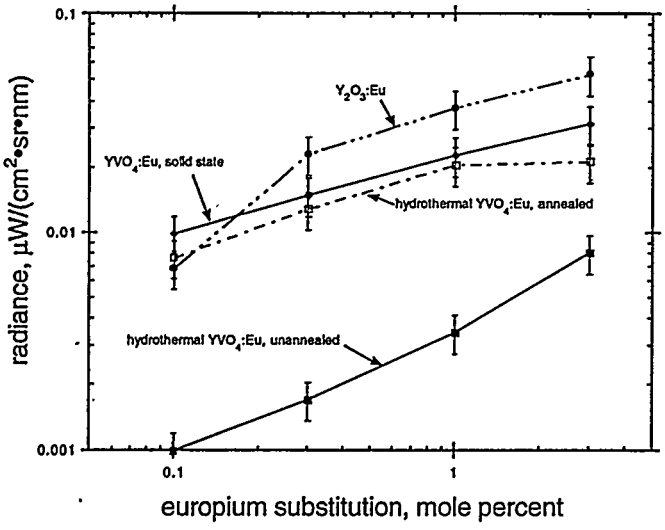

Figure 7. Dependence of maximum CL radiance on activator concentration in hydrothermal YVO_4:Eu, before and after annealing. Data from YVO_4:Eu and Y_2O_3:Eu made via solid state routes (this work) are included for comparison.

This last observation is consistent with Ozawa's explanation of the crystal size effect.[9] When a phosphor particle is irradiated with an electron beam, secondary electrons produced by impact ionization create electron-hole (e-h) pairs in the host lattice. In most CL phosphors, these e-h pairs are free to migrate through the lattice until they encounter a recombination site such as an activator (where they can decay radiatively), or a defect, impurity or grain boundary (where they can decay nonradiatively). Assuming that recombination occurs nearly exclusively at an activator site, the average migration distance of the e-h pair will vary inversely with activator concentration. At lower activator concentrations (or smaller crystal sizes), migration distance and thus activation volume will be limited by crystal size, and at higher concentrations it will be limited by the density of activators. As activator concentration increases to the point where the density of activator ions begins to limit activation volume, CL intensity becomes less sensitive to activator concentration, and the slope of log (intensity) vs log (concentration) diminishes abruptly.

The steep slope of log (radiance) vs. log [Eu] in the unannealed hydrothermal samples indicates that even at activator concentrations as high as 3 mole percent, activation volume is still limited by crystal size. Since the particle sizes of the unannealed and annealed YVO_4:Eu are similar, it is apparent that activation volume is limited by crystallite size, not particle size. This implies that e-h pairs are not capable of crossing grain boundaries without being quenched, and that the principal function of annealing is to eliminate intraparticulate grain boundaries.

An insulating phosphor that is not intimately applied to a conducting substrate will typically show increased intensity with voltage and a threshold of approximately 100-300 V, below which luminescence does not occur.[17] In the sample configuration used in this work, the threshold was generally 200 V, below which surface charging deflected the beam from the sample. Figure 8 shows that even at constant power, increasing beam voltage from 200 V to 800 V increases CL efficiency by a factor of approximately 15.

As was discussed previously, the two principal causes of reduced efficiency at low incident voltage

are surface bound electrons (SBEs) and surface recombinant (SR) centers. It is conceivable that the contribution from SR centers can be reduced by improving crystal quality, but the contribution from SBEs must be dealt with by making the surface of the phosphor grain more conductive. It is not possible to determine from these data the relative influence of SBEs and SR centers at all voltage regimes, though the extreme degree of surface charging seen at the lowest voltages suggests that SBEs are principally responsible for low efficiencies near the threshold voltage.

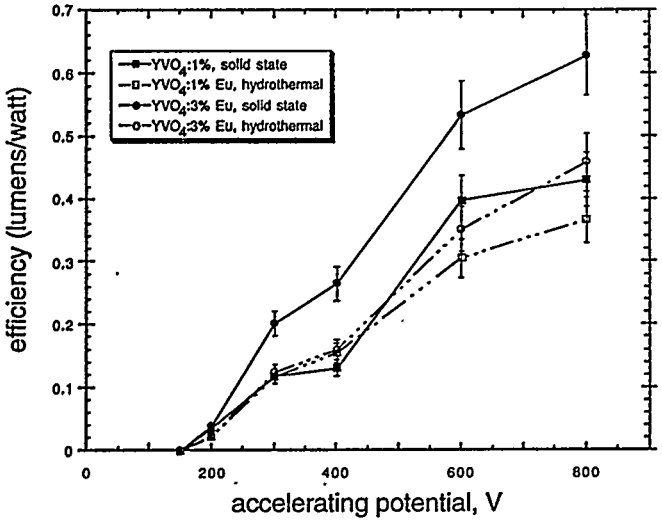

Figure 8: Relationships between electron energy and luminescence efficiency in YVO_4:Eu phosphors prepared using solid state and hydrothermal techniques. Beam power was 15 μW for all measurements.

The highest efficiency observed in a sample of YVO_4:Eu in this work was 0.62 lumens/watt, which was seen in $Y_{0.97}Eu_{0.03}VO_4$ made via solid state and annealed at 1150 °C. Phosphor efficiencies in the range of 2-3 lm/W will probably be required if brightness and power consumption in emissive FPDs are to be similar to those of AMLCD panels.

Other parameters that determine phosphor utility include saturation power and damage threshold. Figure 9 shows luminance from YVO_4:Eu as a function of beam power at 800 V. As current is increased, luminance saturates at approximately 10 mW. If the beam remains focused on the same spot on the sample while the current is decreased, some of the original sample brightness is lost. This hysteresis is shown for a sample of YVO_4:3% Eu made via solid state. This measurement yields essentially the same result for the same composition made hydrothermally (not shown for clarity). The similarity in saturation behavior of solid state and hydrothermal YVO_4:1% Eu is shown in the two lower curves. Once power is increased to the point of saturation, the samples become darkened in the spot where they are irradiated. Within the detection limit of the mass spectrometer (10^{-7} torr equivalent N_2 pressure), no gaseous products were lost from the phosphors during these experiments.

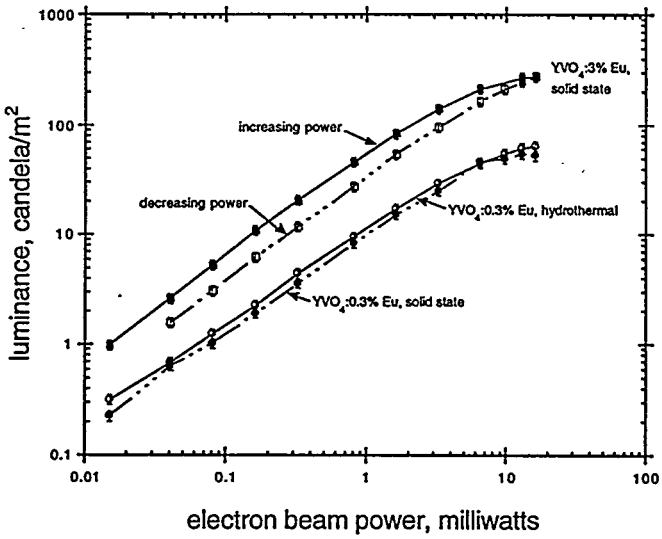

Figure 9: Relationship between luminance and electron beam power in YVO_4:Eu, showing saturation current and hysteresis.

4. SUMMARY

YVO_4:Eu is a capable low voltage oxide phosphor. Though it is slightly less efficient than Y_2O_3:Eu, it has slightly better color saturation, which may allow it to compete with Y_2O_3:Eu for use in low voltage emissive displays. YVO_4:Eu can be synthesized hydrothermally, yielding powders with finer particle sizes than those made from traditional high temperature routes. The powders must be annealed to yield maximum efficiency; however, the modes of the particle size distributions are not affected by annealing. Annealing does not appear to affect the local crystal field of the activator (Eu) ions in YVO_4:Eu, but improves efficiency by eliminating intraparticle grain boundaries, allowing the entire particle to be excited by the incident electron beam. The cathodoluminescent properties

(threshold, efficiency, power saturation) of YVO_4:Eu phosphors appear to be independent of synthetic route. The highest efficiency observed in the YVO_4:Eu samples studied was within a factor of 3.5 of that required to yield a field emitter-type FPD with brightness and power consumption similar to that of an AMLCD panel.

5. ACKNOWLEDGMENTS

This work was supported by the U. S. Department of Energy under Contract No. DE-AC04-94AL85000, and benefited from the talents of Ray Burchard, Robert Mays, and Robert Walko (cathodoluminescence measurements), Bonnie MacKenzie (electron microscopy), Diana Lamppa (particle size analysis), Gary Jones (fluorescence), Mark Rodriguez (X-ray diffraction), and Sherri Heybourne (thermal analysis).

6. REFERENCES

1. L. E. Tannas, Jr., W. E. Glenn, T. Credelle, J. W. Doane, A. H. Firester, and M. Thompson, DARPA ITEC Panel Report on Display Technologies in Japan, June 1992.

2. *a*. I. Brodie and C. A. Spindt, "Vacuum Microelectronics" in *Advances in Electronics and Electron Physics*, P. W. Hawkes, Ed., Vol. 83, Academic Press, San Diego, 1992, pp. 1-106. *b*. C. A. Spindt, C. E. Holland, A. Rosengreen, and I. Brodie, "Field-Emitter Arrays for Vacuum Microelectronics", *IEEE Trans. Electron Dev.* 38(10), 2355-63 (1991). *c*. C. A. Spindt, C. E. Holland, I. Brodie, J. B. Mooney, and E. R. Westerberg, "Field-Emitter Arrays Applied to Vacuum Fluorescent Display", *IEEE Trans. Electron Dev.* 36(1), 225-8 (1989).

3. S. Itoh, T. Tonegawa, T. L. Pykosz, and K. Morimoto, "Influence of Grinding and Baking Processes on the Luminescent Properties of Zinc Cadmium Sulfide Phosphors for Vacuum Fluorescent Displays", *J. Electrochem. Soc.* 134(12), 3178-81 (1987).

4. S. Itoh, T. Kimizuka, and T. Tonegawa, "Degradation Mechanism for Low Voltage Cathodoluminescence of Sulfide Phosphors", *J. Electrochem. Soc.* 136(6), 1819-23 (1989).

5. *a*. S. Itoh, T. Niiyama, and M. Yokoyama, "Influences of gases on the field emission", *J. Vac. Sci. Technol. B* 11, 647-50 (1992).

6. Efficiency data: *a*. K. Narita, A. Kagami, and Y. Mimura, "Behavior of Phosphors under Low Voltage Cathode Ray Excitation", *J. Electrochem. Soc.* 127(8), 1794-98 (1980). *b*. A. O. Dmitrienko and S. L. Shmakov, "The Efficiency of Low-Voltage Cathodoluminescence of Modified Zinc Oxide Crystallophosphors", *Inorganic Materials* 30(4), 534-5 (1994). Threshold voltage: R. E. Shrader, S. F. Kaisel, "Excitation of Zinc Oxide Phosphors by Low-Energy Electrons", *J. Opt. Soc. Am.* 44(2), 135-7 (1954).

7. S. Itoh, H. Toki, Y. Sato, K. Morimoto, and T. Kishino, "The $ZnGa_2O_4$ Phosphor for Low-Voltage Blue Cathodoluminescence", *J. Electrochem. Soc.* 138(5), 1509-12 (1991).

8. A. Vecht, D. W. Smith, S. S. Chadha, and C. S. Gibbons, "New electron excited light emitting materials", *J. Vac. Sci. Technol. B.* 12(2), 781-4 (1994).

9. L. Ozawa, Cathodoluminescence, VCH Publishers: New York, 1990.

10. T. Takamori and L. D. David, "Controlled Nucleation for Hydrothermal Growth of Yttrium-Aluminum Garnet Powders", *Am. Ceram. Soc. Bull.* 65(9), 1282-6 (1986).

11. French Patent 2,007,316 (1970, to Swiss Aluminium Ltd.)

12. T. Takahashi, "Columnar crystalline zinc silicate phosphor prepared by hydrothermal reaction", Japanese Patent 63,196,683 (1988).

13. M. N. Viswanathiah, J. A. K. Tareen, and T. R. Narayanan Kutty, "Hydrothermal Phase Equilibria Studies in Ln_2O_3-H_2O Systems and Synthesis of Cubic Lanthanide Oxides", *Mater. Res. Bull.* 15(7), 855-9 (1980).

14. *a*. R. C. Ropp and B. Carroll, "Yttrium Phosphate-Yttrium Vanadate Solid Solutions and Vegard's Law", *Inorg. Chem.* 14(9), 2199-2202 (1975). *b*. O. Yamaguchi, Y. Mukaida, H. Shigeta, H. Takemura, and M. Yamashita, "Preparation of Alkoxy-Derived Yttrium Vanadate", *J. Electrochem. Soc.* 136(5), 1557-60 (1989). *c*. H. J. Kaunders, "Europium-doped Yttrium Vanadate(V) Phosphor Preparation by Precipitation", U. S. Patent 3,479,296 (1969, to General Electric).

15. R. C. Ropp, The Chemistry of Artificial Lighting Devices, Elsevier: Amsterdam, 1993.

16. R. C. Ropp, Luminescence and the Solid State, Elsevier: Amsterdam, 1991.

17. Insulating phosphors applied to a conductive substrate can luminesce at excitation voltages of less than 50 V, though CL intensities are low. M. T. Anderson, M. L. F. Phillips, and R. J. Walko, "Low-Voltage Cathodoluminescent Properties of Europium-Activated Anion-Deficient Fluorites", *Mat. Res. Soc. Symp. Proc.* 348, 497-502 (1994).

DISCLAIMER